# Polymorphism, Structure, and Chromism in Poly(di-*n*-octylsilane) and Poly(di-*n*-decylsilane)

**W. Chunwachirasiri,† R. West,‡ and M. J. Winokur*,†**

*Department of Physics, University of Wisconsin, Madison, Wisconsin 53706, and Organosilicon Research Center, Department of Chemistry, University of Wisconsin, Madison, Wisconsin 53706*

*Received November 23, 1999; Revised Manuscript Received July 10, 2000*

ABSTRACT: Semicrystalline films and powders of poly(di-*n*-octylsilane) and poly(di-*n*-decylsilane) have been investigated using in situ quenching studies by X-ray scattering and UV−vis absorption in combination with detailed model calculations. These polymers displayed a surprisingly rich array of monotropic and enantiotropic structures during thermal cycling. Poly(di-*n*-decylsilane) was observed to have no less than five distinct ordered forms (crystalline or semicrystalline) which varied in their respective chain structure, packing, and optical properties. Of these only one appeared to be thermodynamically stable. One of the metastable polymorphic structures exhibited an unprecedented tripling of the basic unit cell structure. Poly(di-*n*-octylsilane) samples also exhibited up to five distinct structural forms at temperatures below that of a 25 °C transition to the thermotropic mesophase. Three of these were clearly ordered while the other two are mesophases with features suggestive of a less ordered state. Suggested structural models are used to document and identify the predominant side chain and main chain packing motifs in the various crystalline polymorphs.

## Introduction

Polymorphic behavior is quite common among polymeric and other highly anisotropic materials.[1−3] In many instances the polymorphism seen in polymers requires very specific and, at times, laborious processing conditions. Recent studies of conventional polymers and oligomers have begun to clarify the role that kinetics play in establishing the conditions under which metastable phases may develop.[4−6] While these former attributes are rather general in nature, one exclusive feature that differentiates the $\sigma$-conjugated polysilanes and other $\pi$-conjugated conducting polymers is the delocalization of the electron wave function along the polymer backbone and the profound impact that these structural forms can have on the resulting electronic and optical properties.[7,8] In these latter materials there can be a pronounced interplay between competing molecular level interactions which alter the main chain conformation and, as a direct consequence, the associated interband transition with the appearance of, for example, thermochromism,[9−14] solvatochromism,[15] ionochromism,[16] and piezochromism.[17]

Numerous polysilane studies[18,19] (and references therein) have clearly demonstrated that alkyl side chain substitution creates semicrystalline polymers with varied main chain conformations and thermotropic mesophases exhibiting thermochromism. The shortest symmetric polysilanes (with a monomer unit specified as $-Si[(CH_2)_nCH_3]_2-$ and $n = 0-2$) primarily form crystalline films or powders[20,21] dominated by a nearly planar backbone conformation[22,23] with little or no thermochromism.[24] In di-*n*-butyl ($n = 3$) and di-*n*-pentyl ($n = 4$) substituted materials the net influence of the side chain's bulkiness becomes more pronounced, and there is experimental evidence for a 7/3 helical structure.[25,26] Recent molecular modeling and oligomer studies suggest the existence of backbone conformations intermediate to the well-known anti (i.e., trans-planar, A or $T_0$) and gauche (G) arrangements.[27−29] These new conformations[30] are referred to as ortho (O), "deviant" (D), and transoid[31] (T) with approximate dihedral angles of 90°, 145°, and 170°, respectively (with $T_+/T_-$ and $D_+/D_-$ for both positive and negative helicities). Of these three, an all-$D_+$ (or $D_-$) conformation is qualitatively consistent with a 7/3 helical structure. Side chain packing and crystallization become especially important issues in the longer symmetric dialkylsilanes, and this yields, once again, an all-anti backbone conformation or possibly some form of anti-gauche arrangement.[33] The thermochromism is much more pronounced in these latter samples ($n \geq 3$) with the appearance of a thermotropic mesophase marked by a conformationally disordered arrangement of the Si backbone and a claimed near hexagonal packing of the molecules. This phase is conventionally referred to as a hexagonal columnar mesophase (HCM or, hereafter, just M).

There are also prior reports of crystallographic polymorphism and extremely slow ordering kinetics[32−37] in polydialkylsilanes. This result is not unexpected given the complexity of the main chain conformational energetics in combination with the variations in alkyl packing that can potentially occur. However, the specific details of the main chain and side chain structures are less well established, and in-depth structural refinement studies are sparse.[38−40] Of the many longer ($n \geq 6$) symmetrical polydialkylsilanes, we are aware of only a single crystalline polydihexylsilane (pdHSi) phase, in the work by KariKari and co-workers,[41,42] that has seen full crystallographic powder refinement.

One step in elucidating the full range of structure/property relationships is to simply identify the various structural forms and ascertain what are the key structural attributes in terms of main chain structure, side chain structure, and interchain packing. In the case of the two symmetrical polydialkylsilanes studied in this work, we report on the existence of a large family of

† Department of Physics.
‡ Department of Chemistry.
* To whom correspondence should be addressed.

10.1021/ma9919716 CCC: $19.00 
Published on Web 11/23/2000

monotropic and enantiotropic phases. This structural diversity is paralleled by an equally extensive set of variations in the UV−vis absorption spectra. The paper that follows initially presents a combination of X-ray diffraction and UV−vis absorption data which provide complementary information. X-ray diffraction is primarily sensitive to the intrachain and interchain packing of the alkyl side chains. Since these are chemically anchored to the polysilane backbone, this constrains the main chain conformations. In contrast, the UV−vis absorption is, to first order, insensitive to the specific side chain packing but provides some indication of the overall backbone conformation. Differential scanning calorimetry (DSC) has also been used to characterize these phase transitions.

Thereafter, a series of proposed unit cells and model structures are compared to the X-ray scattering results. These simple models qualitatively clarify many of the underlying structural features although many specific details are not fully resolved. Through this modeling we verify the presence of at least two distinct molecular-level ordering mechanisms, intrachain and interchain. The intrachain ordering processes proceed with relatively rapid time scales while the interchain ordering can require substantially longer times. In all ordered phases there is little or no support for a significant proportion of either gauche or ortho type linkages along the silicon backbone. All low-temperature structures are likely dominated by a combination of the D and T conformations. This paper also presents evidence that the HCM phase itself contains appreciable local ordering closer to that of the low-temperature structures rather than of a more random coillike structure.

## Experimental Details

PdOctSi and PdDecSi were prepared from the corresponding dichlorosilanes by dehalogenation coupling with sodium under standard conditions for polysilane synthesis by Wurtz coupling[43,44] Molecular weights were determined by GPC relative to polystyrene standards: PdOctSi, 1 080 000 ($M_w/M_n$ 3.0), and PdDecSi, 412 000 ($M_w/M_n$ 2.0).

The two primary experimental probes were X-ray scattering and UV−vis absorption. The X-ray data acquisition employed a powder diffractometer mounted to a 15 kW rotating anode X-ray generator (Cu $\lambda_{K\alpha} = 1.542$ Å). This diffractometer used an elastically bent LiF crystal monochromator in combination with a 120° $2\theta$ position-sensitive detector (Inel CPS-120) and full He gas-filled beam paths to minimize absorption and air scatter. Useful scattering data were obtained in the $2\theta$ range of 1.5°−40°. Minimum scan times were on the order of a few minutes, but the data shown typically represent 30−60 min acquisition times. The resolution (full width at half-maximum) of the detector is better than 0.1° ($2\theta$), and upward of 4000 total counts per second were recorded. Individual plotted curves contain up to $10^7$ integrated counts.

For the quenching experiments we employed a simple customized peltier-based heating/cooling stage (200 to −50 °C) suitably modified to accommodate an inlet jet which directed a spray of $CO_2$ powder onto polymer compacted powder or film samples of nominal $1 \times 4 \times 0.5$ mm$^3$ dimensions. The existing design achieved cooling rates in excess of 50 °C/s. This rapid undercooling was especially necessary to stabilize and observe the buried metastable crystalline polymorphs of PdDecSi. For the in situ X-ray studies the quenching chamber was isolated by a pair of thin Be windows.

UV−vis absorption spectra were recorded using a Hewlett-Packard HP8452A diode array UV−vis spectrophotometer. Spectra at various temperatures were obtained from polysilane films deposited on thin quartz microscope coverslips. The general procedure was to first cast films from dilute toluene solution and then wait over 12 h before scanning. The same basic $CO_2$ spray methodology was used to thermally quench the ∼2 $\mu$m cast films. In the UV−vis studies the quenching cell also used quartz windows. X-ray scattering by the as-cast thin films was comparable to that of the precipitated powders. Ultrathin films (under 50 nm)[45,46] have been shown to exhibit reduced crystallinity.

DSC spectra were recorded using a Netzsch model DSC2000. The disparate time scales for the various structural phase transitions complicated implementation of this method. Cooling/heating rates ranging from 1 to 10 °C/min were typically employed. Molecular processes occurring with shorter or longer relaxation times were not well resolved. Quenching was simulated by immersing the aluminum DSC capsules into liquid $N_2$. In this case weak but sharp artifacts, due to condensation of water, were typically observed at 0 °C.

Comparisons with the X-ray scattering data employed structural modeling software based on a custom configured link-atom least-squares (LALS) Rietvelt refinement scheme.[47] To reduce to the effective parameter space of available configurations, the LALS algorithm included a second term, a Lennard-Jones (L-J) hard core packing repulsion ($\propto 1/r_{ij}^{12}$), which constrained the nearest-neighbor distances of the nonbonded C and Si atoms. The actual form of the refinement residual was

$$R = x\frac{\sum_{2\theta}|I^n_{\mathrm{calc}} - I^n_{\mathrm{expt}}|}{\sum_{2\theta} I^n_{\mathrm{expt}}} + (1-x)\sum_{r_{ij}<r_{\mathrm{cut-off}}}^{\text{unit cell}} \frac{a_{ij}}{r_{ij}^{12}}$$

where the relative contribution, $x$, and the L-J scaling coefficients, $a_{ij}$, and the $r_{\mathrm{cut-off}}$ were arbitrarily determined. Analogous procedures have proven helpful in studies of other polymers.[48] By selectively increasing and decreasing the relative contribution of these two components, trapping in many local minimum was avoided. The exponent $n$ was typically chosen to be either $^1/_2$ or 1 to alter the relative weighting of the peak intensities. We note that while the specifics of the chosen background profiles and the various aforementioned fitting parameters are subjective, this procedure can rigorously avoid physically impossible structural variations. In general, the background profiles at wide angle (about $2\theta = 20°$) had a smoothly varying line shape intermediate to that of the high-temperature mesophase and the quenched samples. Enhancements in the modeling algorithm are still necessary for further optimization of the structural refinements.

The choice of the representative polydialkylsilane unit and intrachain degrees of freedom was also important aspects of the structure refinement process. Since the oriented film studies of ref 33 clearly delineate a nominal 7.8 Å repeat along the chain axis, a chain repeat employing four $SiR_2$ monomers was adopted. A longer chain sequence is necessary to more accurately explore the 7/3 helix which is often cited. For this work bond angles and bond lengths were generally kept rigid while the dihedral angles were allowed to vary over a large range of angles. At first the side chains were constrained into four functionally independent pairs (of the eight), but once the calculated structure factor bore some resemblance to the experimental data, all eight side chains were allowed to reorient freely. No attempt was made to introduce intrachain energetics. In general, little or no improvements in the $R$ factors were obtained for changes in the dihedral angles at or near the terminating methyl group at the side chain ends. As a consequence, these were fixed to an anti conformation, and only changes in the Si−C and four (or five) C−C linkages nearest the backbone were freed. This treatment is consistent with the proposed side chain packing for poly(di-*n*-tetradecylsilane).[33] The actual resemblance to real, energetically favorable conformations may therefore be marginal. This process however does allow the side chain to, on average, point in an appropriate direction and, because of the hard-core packing constraints, move in an orchestrated fashion. Specific details

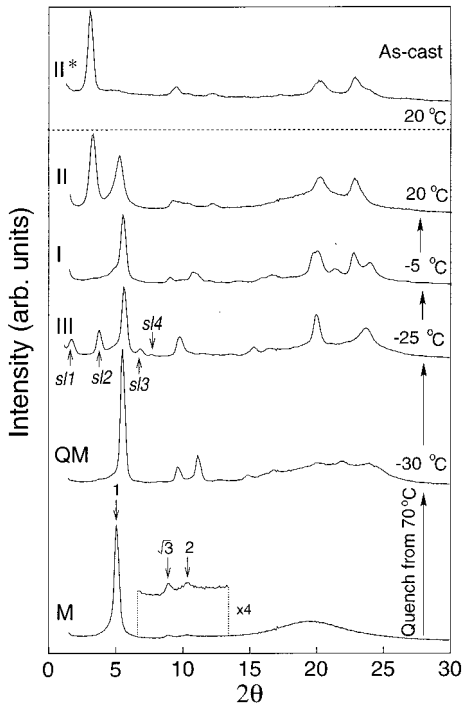


**Figure 1.** Representative powder diffraction profiles from the four crystalline polymorphs of PdDecSi seen during thermal cycling from the high-temperature mesophase. A fifth crystalline form (type II* at top) is observed only during casting from solvent. All curves have been offset for clarity.

of the side chain and main chain structures are likely to be in error, but the overall "average" chain attributes should have qualitative merit in the discussion that follows. All atomic species, C, H, and Si, were included in the structure factor calculations. Of these, clearly the contributions by the carbon and silicon atoms dominate, but disregarding the hydrogen may lead to undesirable systematic errors.

## Experimental Results

**A. Poly(di-*n*-decylsilane) X-ray Scattering and UV−vis Absorption.** Figure 1 displays, for PdDecSi, six essentially "single"-phase X-ray scattering profiles for the various claimed phases and their designations. PdDecSi can be thermally cycled or solvent cast to form at least five nominally crystalline polymorphs. They are hereafter referred to type II*, I, II, III, and QM (for quenched mesophase). Of these, only two phases, I and II, are explicitly cited in the literature.[33,36] Intermediate X-ray spectra (not shown) exhibited a simple coexistence of two ordered structural phases, one of which, at the appropriate temperature regime, exhibited a monotonic increase in intensity while the other smoothly decreased. These data also contain scattering features indicative of a small portion of noncrystalline material. The time evolution of the X-ray scattering was sensitive to both temperature and thermal history. This latter topic, crystallization kinetics and growth, will appear in a separate publication and therefore is not discussed in depth here.

PdDecSi phases I and III appear to be monotropic[49] while the type II structure is clearly enantiotropic. The QM form may be only representative of a kinetically limited structure and so cannot be assigned. The QM phase can be warmed to sequentially give the type III, type I, and, finally, type II structures (using the nomenclature of Mueller et al.[36]). This sequence is irreversible because each ordered phase, once formed,

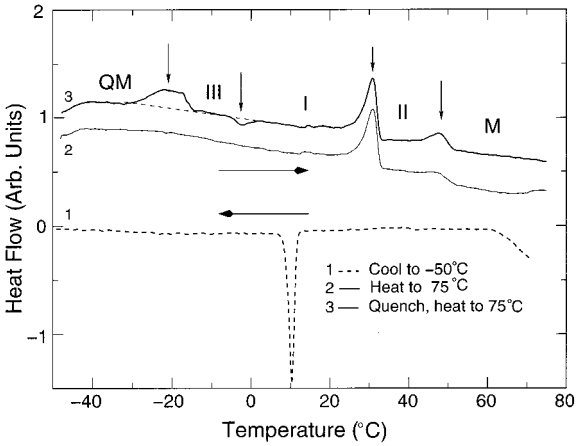


**Figure 2.** Selected DSC curves, at heating/cooling rates of 5 or 10 °C/s, for PdDecSi after modest cooling and after quenching (from 70 °C). The top two curves have been slightly rescaled and offset.

does not revert back to its prior form on cooling. The type II* structure is metastable and only appears during solvent casting or precipitation of PdDecSi (in this instance using toluene) and has a very distinctive low $2\theta$ angle scattering profile and packing motif. This latter attribute will be shown later to have significance for justifying the postulated interchain packing of the type II phase.

Selected DSC thermograms are shown in Figure 2. In general, one strong exotherm was seen on cooling while two (or sometimes three) endotherms were typically resolved on heating. The relative intensity ratios were very sensitive to the specified sweep rates and thermal histories. The exotherm seen on cooling corresponds to transformation from the high-temperature mesophase (M) to the type I form. The very slow kinetics of the M → II transformation obscure its signature. In the initial heating run (labeled 2) these two endothermic peaks are identified as "melting" of the type II and type I fractions. The presence of significant, sweep-rate-dependent, hysteresis is typical of polymer samples. However, the presence a possible third peak (not shown) suggests that the "disordering" of type I phase proceeds through a two-step process with the formation of a transient intermediate structural state. Quenching, followed by heating, produces at least two new features. The first is a broad endotherm centered near −22 °C, and the second is an exotherm near −2 °C. The first corresponds to the QM → III transition while the second is suggestive of a cold crystallization process in the transformation from the type III to the type I phase.

With respect to the X-ray data in Figure 1, an equivalent progression of the PdDecSi UV−vis absorption spectra is shown in Figure 3. Simultaneous X-ray and UV−vis measurements were not possible due to incompatibilities in the required sample dimensions and instrumentation. Although thermal histories were kept as consistent as possible, the respective data sets had temperatures that commonly varied by a few °C. The distinctive changes in the polymer structure are paralleled by equally dramatic changes in the UV−vis absorption. In general, intermediate data, as shown in the inset of Figure 3, typically exhibited one or more isosbestic points. This typically implies that the structural evolution also proceeded through a simple two-phase coexistence. The slow, stepwise progression of temperatures during the UV−vis data acquisition would

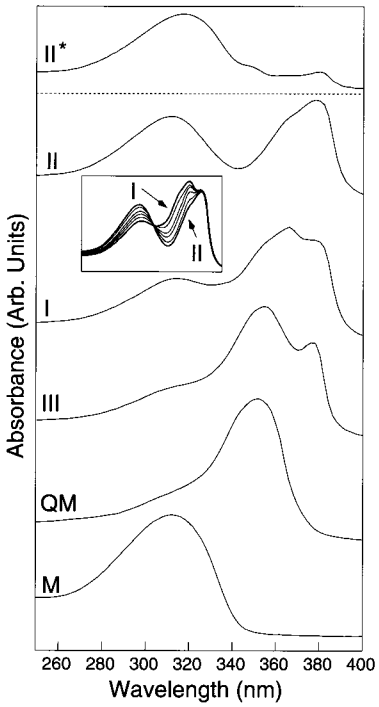


**Figure 3.** Representative UV−vis absorption spectra from the four crystalline polymorphs of PdDecSi seen during thermal cycling from the high-temperature mesophase. A fifth crystalline form (type II* at top) is observed only during casting from solvent. All curves have been offset for clarity. Inset: the full set of data recorded during the type I → type II transition.

not be expected to resolve the presence of a transient, intermediate state. It is also important to note that the presence of multiple UV−vis absorption peaks in PdDecSi may originate from a single structural phase. The X-ray scattering data are unequivocal in delineating a stepwise progression of distinct structural phases on slow heating.

Referring back to Figure 1, the high-temperature mesophase scattering profile (at bottom) includes three arrows. These are used to identify the position of the first three sharp features whose relative wave vector positions are approximately in the ratio of $1:\sqrt{3}:2$ (appropriate for a 2-dimensional triangular lattice). Immediately above this curve is the scattering profile of the QM form. While the QM phase peaks are quantitatively different from those of the M phase, they still include three analogous lower angle reflections with the same nominal wave vector ratios. This suggests that the general interchain packing of the QM is comparable to that of the HCM. The lack of strong distinguishable peaks, as compared to the type I, II, II*, and III phases, at higher $2\theta$ angles implies that ordering of the alkyl side chains has been strongly suppressed by the rapid cooling. Alkyl side chain substituted polymers that include appreciable side chain ordering typically display sharp scattering peaks at $2\theta$ positions qualitatively comparable to the (110) and (200) reflections of crystalline alkanes or polyethylene.[50]

Despite the observation that the QM and M phases have qualitatively similar X-ray profiles (and, by conjecture, interchain packing), it is apparent that the average Si backbone conformation is drastically different. The QM phase of PdDecSi exhibits essentially a *single* narrower absorption maximum centered at 352 nm. Typically a persistent weak shoulder in the vicinity of 310−320 nm remains in all low-temperature spectra. The relative intensity of this feature increases with respect to each passing structure (i.e., QM → III → I → II). Naively, this may be attributed to a stepwise increase in the proportion of less-ordered regions of polymer. However, there are no clear-cut features in the X-ray data indicative of this process (at least not at the three lowest temperatures).

The QM phase is sequentially followed, on heating, by the metastable type III structure. The most intense peak, centered near $2\theta = 5.6°$, is retained, but all other peak positions bear little resemblance to those of the QM phase. Of particular interest are the appearance of four new peaks (*sl*1 to *sl*4, *sl* ≡ superlattice), two at lower $2\theta$ angles of 1.9° and 3.85° and two at higher angles of 6.9° and 7.75°. These new peaks have widths and profiles comparable to the other scattering features. This behavior suggests that they are intrinsic components of the type III unit cell. The low angle *sl*1 and *sl*2 features imply formation of a larger repeat with new *d* spacings of 4.65 and 2.30 nm, and as the modeling section will demonstrate, these features are consistent with a uniaxial tripling ($3 \times 1$) of the basic unit cell structure within the equatorial plane. While such processes are often seen in intercalation compounds[51] or by reconstructions at crystal surface interfaces they are not often observed in nascent homopolymers. There are also two clearly distinguishable peaks at $2\theta = 20.1°$ and 23.7° superimposed on the "amorphous" background scattering halo which is now centered about $2\theta = 21°$. Hence, the type III phase must also include appreciable interchain ordering of alkyl side chains.

The UV−vis absorption spectrum for this type III phase develops a new peak near 378 nm and a slight increase in the 310 nm shoulder. This indicates that some regions of the polymer have increased planarity (peaks near 380 nm are typically associated with an all-anti conformation), and some regions have reduced planarity and/or increased main chain disorder.

At higher temperature the type III phase transforms to the known type I phase with no residual trace of the superlattice peaks. The type I pattern is actually qualitatively most similar to that of the QM phase at lower $2\theta$ angles. This signifies that the average interchain packing is retained throughout the QM → III → I sequence. However, there are distinctive changes at wider $2\theta$ angles with a minimum of at least four distinguishable scattering peaks at $2\theta$ angles above 20°. This implies evolution in the overall packing of the alkyl side chains as well. Changes also occur in the UV−vis absorption spectrum with a continued increase in the 310 nm shoulder (now a peak nearer 313 nm) and the presence of a distinguishable peak centered near 365 nm.

Finally, at temperatures above 0 °C, the originally quenched PdDecSi sample undergoes one last crystal−crystal transition to the type II phase. As discussed in the recent report of Mueller et al.,[36] this transition is very sluggish. The scattering profile for this phase is markedly changed from that of the type I structure with fewer distinguishable reflections and significantly different $2\theta$ positions. The new low angle peak at 3.2° is quite strong and identifies a new interchain 2.76 nm *d* spacing. The UV−vis also continues to evolve with, as best seen in the inset of Figure 3, a continued increase in the 313 nm peak and an intensity loss of the 365 nm absorption feature. The 378 nm peak remains unchanged.

After extended annealing times there are no scattering features indicative of any residual type I phase. However, one may claim that the broader peak centered at $2\theta = 5.4°$ reflects the presence of a significant proportion of a HCM-like phase which forms after warming the metastable type I phase above some threshold temperature before passing on to the thermodynamically stable type II structure. NMR studies, by Mueller and co-workers,[36] resolve a narrow peak that is consistent with this scenario. In fact, if the $2\theta = 5.4°$ peak is excluded, then the type II scattering profile bears a resemblance to the type II* scattering profile shown at the top of Figure 1.

As noted previously, the type II* polymorph appeared during casting from solution. Its pattern is noticeably different because it contains a single relatively narrow peak at $2\theta = 3.4°$ and only a very weak broad feature centered near $2\theta = 5°$. There are additional less pronounced components at higher $2\theta$ angles as well. This clearly indicates dramatic changes in the interchain packing of the type II* structure. The UV−vis absorption is also striking (at top in Figure 3) because this profile is dominated by a single broad peak with a $\lambda_{max}$ of 318 nm. While there are weaker features near 350 and 380 nm the implication is that, overall, the II* phase adopts a conformation different from all other crystalline forms.

If the type II phase truly represented a superposition of type II* phase and a M-like phase, then one would expect the UV−vis absorption to be dominated by a *single* peak centered *below* 320 nm. The type II profile, shown in Figure 3, is clearly inconsistent with this scenario. Alternatively, one might claim that this "M"-like phase is actually associated with the long wavelength absorption feature. (The following PdOctSi results will show that this novel idea may actually have merit.) On closer inspection we note that there are small but noticeable discrepancies in the peak positions of type II and II* diffraction profiles. Moreover, the clear isosbestic point seen in the inset of Figure 3 during the type I → II transition is more consistent with formation of a single, heterogeneous type II phase after prolonged annealing. At present a single type II phase seems more likely.

**B. Poly(di-*n*-octylsilane) X-ray Scattering and UV−vis Absorption.** Figure 4 contains the best representative "single"-phase X-ray scattering profiles and specific sample thermal history for PdOctSi. Although there are similarities to some of the PdDecSi spectra, the actual thermal progression in PdOctSi appears even more complicated. PdOctSi yielded at least three ordered structures, and these are referred to as QM, I, and II. All three appear to have qualitatively similar analogues in the literature.[33,37,52] PdOctSi samples evidence two additional structures which are, from their X-ray spectra, reminiscent of the higher temperature thermotropic mesophase, type M, and so are designated M′ and M″. This M′ phase can best be distinguished by other characterization methods. Isolating the claimed M″ was especially problematic because it is transient and only appeared as a minority phase in PdOctSi during the type I → II transition. Assuming solely a simple two-phase superposition of the type I and II phases does not fit the indicated M″ profile.

For this PdOctSi sample the type II structure is monotropic and appears only after warming from either the QM or type I phases above 10 °C. In the latter

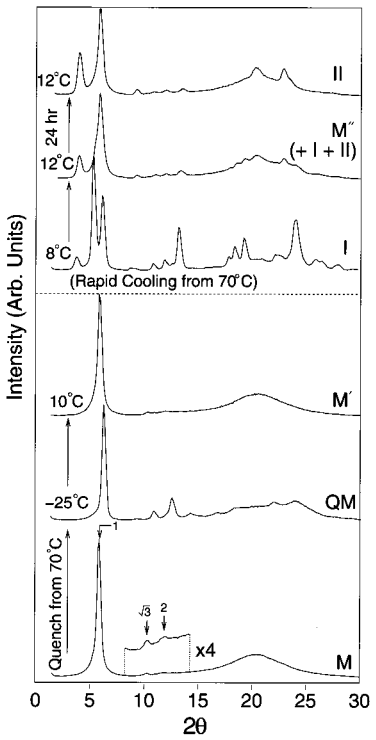


**Figure 4.** Representative powder diffraction profiles from the various polymorphs of PdOctSi during thermal cycling from the high-temperature mesophase. Top: structural phases observed after rapid cooling to 8 °C. Bottom: scattering data observed during a low-temperature quenching cycle. All curves have been offset for clarity.

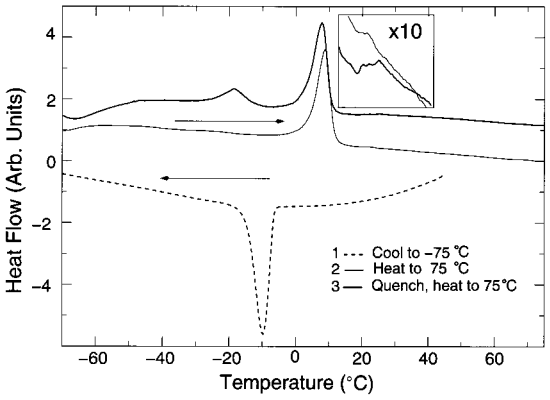


**Figure 5.** Selected DSC curves, at heating/cooling rates of 5 or 10 °C/s, for PdDecSi after modest cooling and after quenching (from 70 °C). The top two curves have been slightly rescaled and offset.

instance this process occurs extremely slowly. The PdOctSi type I phase itself forms only on *cooling* from the mesophase within a narrow temperature window spanning from 5 to 10 °C. The precise conditions for formation of the M′ and M″ phases are not fully clarified. In this study the M′ phase was only observed on heating, but there is evidence that this phase may also form on cooling at sufficiently slow cooling rates.[37] The PdOctSi type II and M′ structures both appear thermally stable at up to 25 °C. Thus, the reported 10 °C crystal−HCM transition[37] represents alternative structural pathways (on heating, either QM → M′ or I → M″).

Example DSC thermograms are shown in Figure 5. In general, only one large peak was seen on either cooling or heating. Because of the relatively slow kinet-

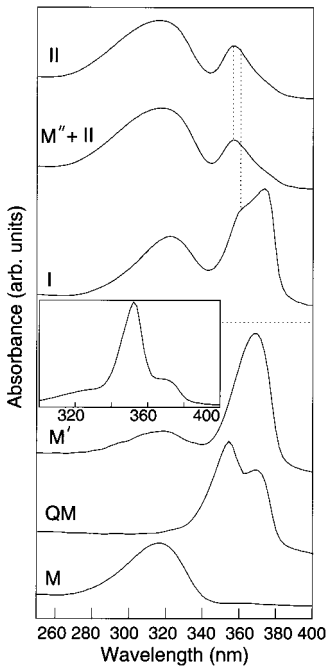


**Figure 6.** Representative UV−vis absorption spectra from the various polymorphic forms of PdOctSi during thermal cycling from the high-temperature mesophase. Top: structural phases observed after rapid cooling to 8 °C. Bottom: scattering data observed during a low-temperature quenching cycle. Inset: final UV−vis absorption spectrum after rapid cooling to 0 °C. All curves have been offset for clarity.

ics associated with the formation of the type I or II phases, the −10 °C exotherm on cooling is correlated with formation of the QM phase while, on heating (and labeled as curve 2), the +10 °C endotherm corresponds to a transformation to the M′ phase. The expanded the vertical scale of Figure 5 (inset) identifies a much weaker, but reproducible, endothermic peak occurring just above 20 °C. Clearly, melting of the side chains (at 10 °C) involves substantially more entropy than does the disordering of the silicon backbone (at 20−25 °C). Work by Kanai et al.[37] and others[53] also resolve these features. Additionally, a very weak endotherm near −20 °C is reported. Quenching, again by immersion of the warmed aluminum DSC container into liquid $N_2$, significantly increases the relative intensity of the third endothermic peak near −20 °C. This feature is correlated with the formation of the single 373 nm peak in the PdOctSi UV−vis absorption. At slower cooling rates, 1 °C/min (not shown), a weak exotherm could be observed near +8 °C, which is suggestive of marginal formation of the type I phase.

Representative UV−vis absorption spectra, in this case for PdOctSi, are shown in Figure 6, and once again, there are dramatic changes in the UV−vis absorption with, in many instances, multiple absorption features. Initially the QM phase of PdOctSi exhibits two peaks centered near 355 and 373 nm. In the case of PdDecSi all spectra contained a persistent shoulder in the vicinity of 310−320 nm which could, in part, be attributed to residual, less-ordered (i.e., amorphous) regions of polymer. Thus, the overt lack of a shoulder in the PdOctSi QM absorption spectrum is an enigma and, by its absence, indicates that this short wavelength feature may have an entirely different origin altogether.

With the exception of the M → QM quench, the progression of the PdOctSi QM phase on heating differs from that of PdOctSi. Because of the slower kinetics, rapid quenching of PdOctSi is unnecessary, and a QM-like structure has been observed previously[37] at a cooling rate of 10 °C/min. As the temperature is raised above 10 °C, the QM phase X-ray scattering profile nominally reverts back to that of the M phase. Hence, the UV−vis absorption spectrum for this PdOctSi film is remarkable because it is clearly dominated by a single, moderately broad absorption feature at 372 nm. There is also a much weaker peak centered at 320 nm. This result demonstrates that a HCM-like phase, designated M′, can develop while having a significantly different and far more planar backbone conformation. A preliminary finding is that suppression of side chain crystallization may also lead to improved $\sigma$-conjugation. The UV−vis absorption reverts to that of the M phase at temperatures above 25 °C. Since the side chains are already disordered, disordering of the backbone requires relatively small changes in the overall entropy, and this would involve only a very small latent heat.

Only one of the other two designated crystalline phases of PdOctSi, type II in Figure 4, has an X-ray scattering profile which bears a qualitative resemblance to that of PdDecSi. There are also pronounced differences in the thermal pathways as well. Preparation of the type I form, within its narrow temperature window, is always accompanied by a small quantity (in this case under 10%) of the type II phase. Hence, direct comparisons are difficult without referring to the modeling calculations that follow. The PdOctSi type I and II phases both include extensive side chain ordering with, in the case of the thermodynamically stable type II phase, a low-angle scattering peak suggestive of a fundamentally different chain-to-chain packing scheme. The PdOctSi type I X-ray pattern is also quite unusual for the large number of distinguishable reflections, measurable Bragg scattering out to $2\theta = 40°$, and splitting of the generic $2\theta = 5°$ peak into two narrowly separated components. The type I UV−vis absorption shown in Figure 6 qualitatively resembles that of the PdDecSi type I phase with a broad peak at 320 nm and two additional peaks centered near 360 and 375 nm. Primarily on the basis of X-ray film studies of oriented fibers, KariKari and co-workers[33] assign an all-anti conformation to this phase. With respect to the UV−vis absorption, a proportion of the PdDecSi type I phase is consistent with an all-anti backbone conformation, but a significant fraction of this sample includes less planar backbone structures as well.

Warming the type I PdOctSi, above 10 °C, initiates a pronounced decrease in the absorption of the longer wavelength features in conjunction with an increase in the "320 nm" peak intensity (and a 5 nm shift to shorter wavelength). This is subsequently followed by a subtle and much slower intensity increase of a single peak in the vicinity of 357 nm. None of these absorption spectra so far are fully consistent with those reported by Kanai et al.[37] Rapid cooling, to temperatures ranging between 0 and 5 °C, provides yet another possible outcome (shown in Figure 6, inset), and this UV−vis absorption does match that of ref 37. The relationship of this last result to other structural attributes is still under investigation.

**C. Structural Modeling.** Modeling establishes a framework for further discussion of the predominant structural characteristics. The type I structures, shown in Figure 7a,b, are treated first because they are

**Table 1. Calculated Unit Cell Parameters for the Various Structural Phases**

| | lattice repeats (nm) | | | angles (deg) | | | | |
|---|---|---|---|---|---|---|---|---|
| polymer/phase | *a* | *b* | *c* | α | *β* | *γ* | chains (unit cell) | density (g/cm$^3$) |
| PdDecSi I | 2.79 | 1.69 | 0.79 | 98 | 89 | 144 | 1 | 0.96 |
| PdOctSi I | 2.27 | 1.63 | 0.795 | 96 | 91 | 142 | 1 | 0.95 |
| PdDecSi II* | 2.91 | 0.98 | 0.79 | 105 | 104 | 94 | 1 | 0.98 |
| PdDecSi II | 2.75 | 2.02 | 0.79 | 105 | 102 | 94 | 2 | 0.97 |
| PdOctSi II | 2.23 | 1.97 | 0.79 | 105 | 91 | 95 | 2 | 1.01 |
| PdDecSi III | 8.54 | 1.67 | 0.795 | 100 | 90 | 146 | 3 | 1.02 |
| PdDecSi QM | 3.07 | 1.79 | 0.79 | 92 | 93 | 149 | 1 | 0.93 |
| PdOctSi QM | 2.86 | 1.65 | 0.79 | | | 150 | 1 | 0.91 |
| (hexagonal) | 1.65 | 1.65 | 0.79 | | | 120 | 1 | 0.91 |

commonly reported elsewhere[36] (after moderate cooling from the thermotropic mesophase), and these scattering profiles have a significant number of resolvable reflections. In addition, they have been tentatively assigned orthorhombic unit cells containing two polymer chains and $T_0G_+T_0G_-$ (in PdDecSi) or all-anti (in PdOctSi) main chain conformations in ref 33. As noted earlier, most scattering peaks at $2\theta$ angles under 19° are primarily equatorial (*hk*0) in nature while many of those at higher angles are correlated with ordering of the side chains and are often nonequatorial. Hence, the three main peaks, in PdDecSi and PdOctSi, near 20°, 23°, and 24° yield *d* spacings of 0.44, 0.39, and 0.37 nm, respectively, values consistent with interchain spacings seen in crystalline alkanes and polyethylene.[50]

For the PdDecSi sample, which had been quenched prior to heating, the wave vector of the first three observed peaks (at 0.39, 0.65, and 0.77 Å$^{-1}$) and, as noted earlier, roughly approximates a ratio of 1:$\sqrt{3}$:2. This is suggestive of a near hexagonal packing of the polymer chains with a 1.86 nm repeat. Assuming a hexagonal packing with this repeat yields a calculated mass density under 0.89 g/cm$^3$, which is somewhat too low be physically realistic. Modeling calculations (not shown) using a rigorously hexagonal construction or the unit cell of ref 33, in combination with a $T_0G_+T_0G_-$ Si backbone or other configurations, are unsatisfactory for either indexing the main scattering peaks or obtaining a reasonable match to the experimental scattering intensities.[54]

There are a few telltale features in the PdDecSi data (and the PdOctSi data as well) which cast into doubt the presumption of hexagonal packing. Inspection of the third "sharp" peak, at $2\theta = 10.9°$, indicates a shoulder on the high angle side and, hence, a superposition of two partially overlapping peaks. Reasonable agreement in both peak positions and intensities is obtained using a triclinic unit cell[55] specified in Table 1. This single chain unit cell is close to a two-chain orthorhombic approximate of $2.79 \times 1.95 \times 0.79$ nm$^3$. It is important to reemphasize that with a limited number resolved reflections (as compared to molecular crystals) the uniqueness of a given structural model is suspect although other structural models are likely to have many of the same overall features. The known chemical linkages and architecture represent a significant set of constraints. We also find that small orchestrated changes in the unit cell dimensions can be accommodated by systemic variations in the local polymer structure. This can alter the specific indexing of the nonequatorial peaks.

The most important aspects of this modeling are the description of the general Si backbone conformation, the alkyl chain orientation and packing, and the overall chain-to-chain packing. From a modeling perspective it is unlikely that a $T_0G_+T_0G_-$ backbone conformation can be accommodated to any great extent. In the case of PdDecSi any $T_0G_+T_0G_-$ conformation simply *cannot* span the nominal 28 Å *a*-axis repeat. The specific model used in Figure 7a has two Si backbone dihedral angles (of the four) which deviate, on average, ±20° from planarity. Given this result, we suggest that the Si backbone is dominated by T[56] and D conformers with an $T_nD_-T_{n'}D_+$ construction (with small integer values of *n* and *n*′) which includes considerable conformational disorder both along the backbone and within the side chains (a *condis* crystal[57]). A sequence of this kind would have three basic Si environments with a Si surrounded by two T linkages, a T and a $D_+$ (or $D_-$), or even a $D_+$ and $D_-$, a result qualitatively consistent with solid-state NMR studies.[36]

The major observation, with respect to this side chain construction, is that ordering occurs first and foremost along neighboring alkyl chain pairs along opposite sides of a single polymer chain, as shown in Figure 8a, and then coordinates with the alkyl units of neighboring chains. This motif contrasts very strongly with the interdigitated nesting seen in polydihexylsilane[41] (pdHSi) and schematically depicted in Figure 8b. Recent studies of tetra-*n*-alkylammonium salts[58] demonstrate a similar crossover, from a so-called "tetraradial" to a "biradial" construction, in their alkyl chain packing when the side chains are close to 12 carbon atoms in length. Calculations of the packing energy have shown that correlated pairs of gauche linkages occur near the core nitrogen atom, thereby enabling structural registry of adjacent alkyl chains. Our, admittedly primitive, modeling exhibits some similarities. The basic PdDecSi structural packing unit therefore resembles a "bow-tie" shaped object as shown in Figure 7a (inset) which packs laterally in the type I phase as staggered bricks in a wall. Although the unit cell specified in Table 1 highlights the lamellar aspects of this construction, there is also an underlying near hexagonal packing of Si backbones which maps onto the high-temperature HCM phase.

The PdOctSi type I phase data,[52] shown in Figure 7b, appear to differ from that of PdDecSi because there are now two closely spaced peaks at 5.5° and 6.4° and a surprisingly large number of peaks present at higher angles. In addition, a small percentage of the type II structure introduces distinct scattering artifacts at $2\theta = 4.2°$ and 5.9° and much weaker features elsewhere. Shortening the side chain by two $CH_2$ units, to give an octyl branch, alters the equatorial aspect ratio of the polymer host. This effect is paralleled by analogous changes in the equatorial unit cell repeat along the *a*-axis direction. Combining the basic "bow-tie" building block of Figure 8a with the proposed type I packing scheme also yields reasonable refinements to the ex-

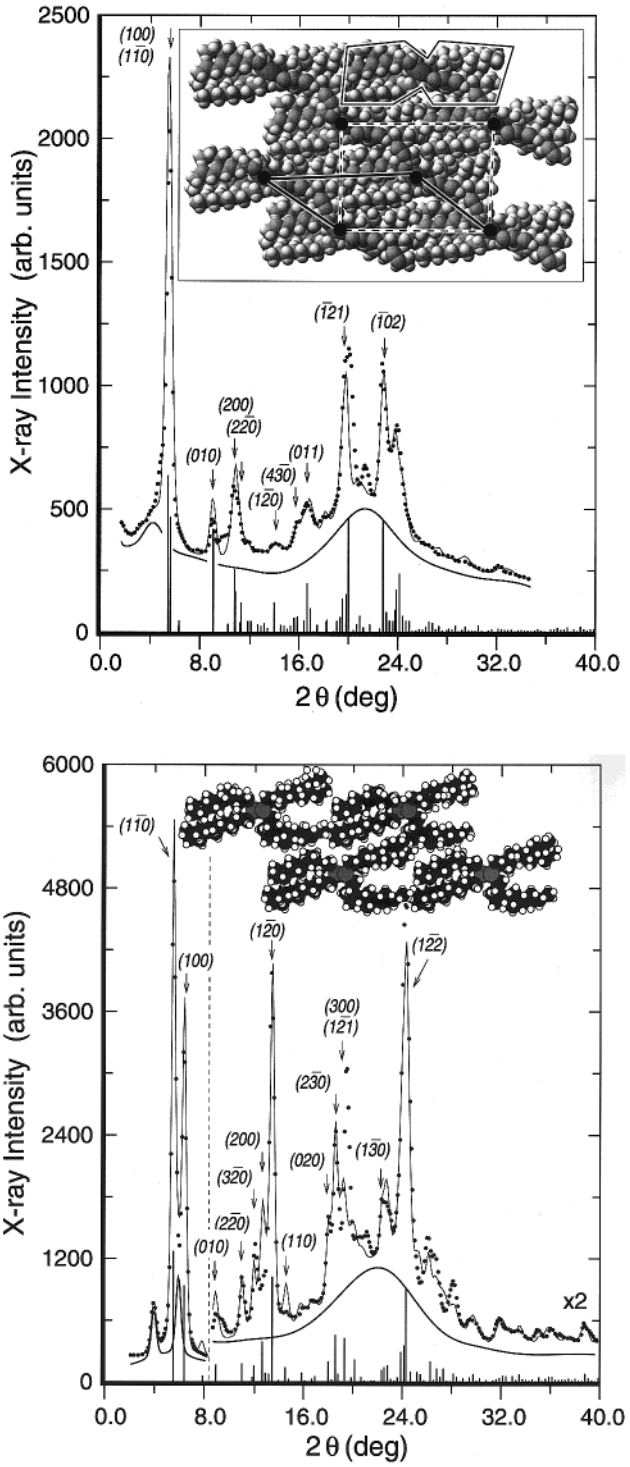


**Figure 7.** Comparison of the calculated powder profile (thin line) and experimental data (filled circles) for the type I phase of (a, top) PdDecSi and (b, bottom) PdOctSi using the model, as viewed along the chain axes, in the respective insets. The specific unit cell parameters are given in Table 1. In addition, each of these figures includes an arbitrary background profile (thick line) and the underlying Bragg contributions (as thin vertical bars).

perimental data in both position and, for the most part, intensities. Discrepancies are still present in both these claimed type I models (and in the additional data sets that follow). Thus, some aspects of the local ordering are incomplete. The UV−vis absorption results clearly suggest that these crystal "phases" incorporate more than a single backbone conformation, and so, at the very least, a more accurate model should make allowances for this attribute. Our assumed unit cell construction will tend to interpolate between these related structural forms.

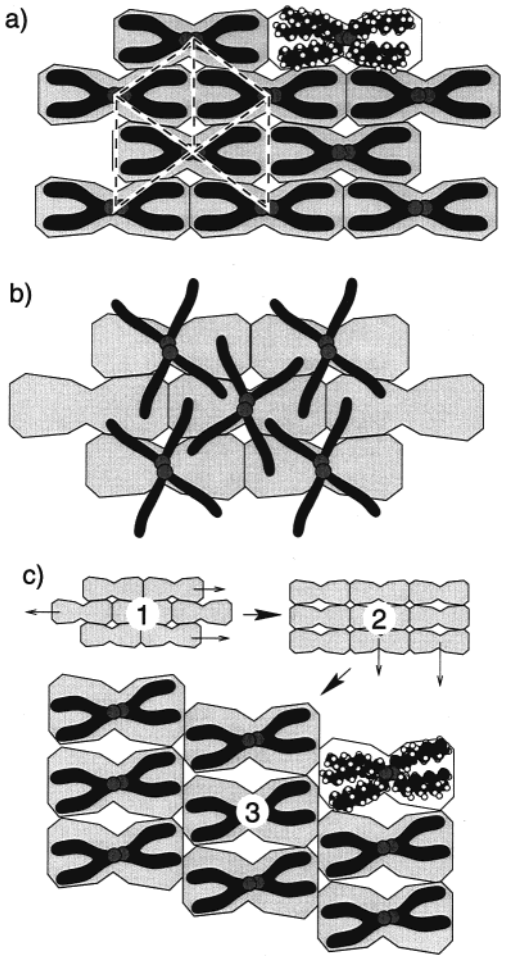


**Figure 8.** (a) Schematic of the proposed interchain packing motif adopted by the type I phases of PdOctSi and PdDecSi. (b) Schematic of the intrachain and interchain packing proposed in ref 41 for crystalline PdHSi. (c) Schematic of the proposed interchain packing motif adopted by the type II* phase of PdDecSi in combination with its relationship (via the sequence 1 → 2 → 3) to the type I phase of (a).

The specific lattice constants are again given in Table 1 and approximate a two-chain orthorhombic cell with dimensions of 2.28 × 1.96 × 0.79 nm$^3$. With respect to the specific details of the PdDecSi model, the refined model structure in PdOctSi appears to contain a somewhat less uniform packing of the alkyl side chains within a single polymer chain entity. Hence, PdOctSi is likely situated near or at a crossover regime between the noninterdigitated "biradial" construction of PdDecSi and the nested structure of PdHSi. These differences may have important implications for the crystallization kinetics and, in part, be responsible for the distinctive variation in the low-temperature structural phase behavior between PdOctSi and PdDecSi. Analogous studies of quenched PdHSi would help address this issue.

Prior to discussing the other known class of PdOctSi and PdDecSi crystalline polymorphs, the type II form, the peculiar metastable type II* phase is introduced because this phase represents another limiting case for the interchain packing and leads naturally into a discussion of the proposed type II packing. As shown in Figure 9, the low-angle region of the type II* phase

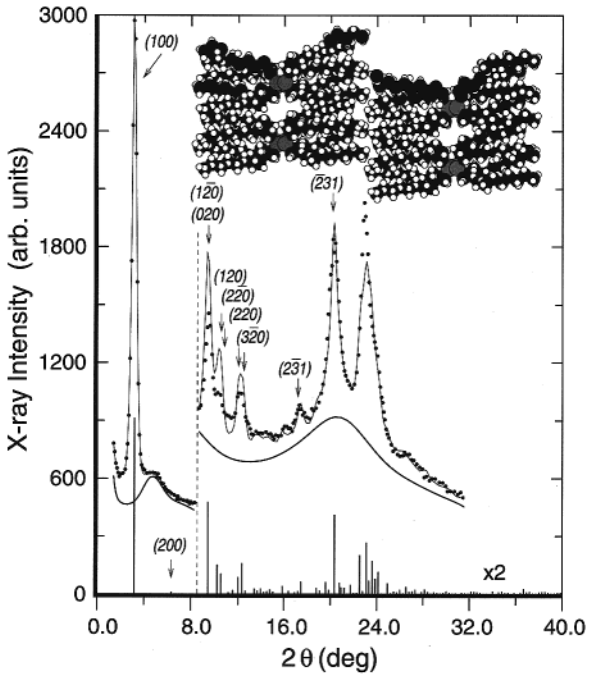


**Figure 9.** Comparison of the calculated powder profile (thin line) and experimental data (filled circles) for the type II* phase of PdDecSi using the model, as viewed along the chain axes, in the inset. This figure also includes an arbitrary background profile (thick line) and the underlying Bragg contributions (as thin vertical bars).

scattering is dominated by a *single* sharp peak at $2\theta = 3.4°$ and only a broad feature centered near 5°. The latter is most likely due to the scattering from noncrystalline regions of the polymer film which approximate the packing of the type I form. Modeling of these data referenced a single chain unit cell of nearly equal dimensions to that of the type I structure but with a strikingly different packing motif depicted in Figure 8c. Qualitatively, these two motifs differ by a pair of translational displacements of the polymer chains within the equatorial plane. With this construction there is considerable open space in the region immediately adjacent to the silicon backbones. As such, it is likely that PdDecSi can include increased main chain conformational disorder, and this would lead to a net shift to lower $\lambda$ of the interband transition maximum. The UV−vis spectrum of this phase is very sensitive to temperature variations even though there are no distinctive changes in the diffraction pattern until 25 °C, at which point it transforms into the HCM structure.

The type II phase structures, referring back to Figures 1 and 4, exhibit a limited number of new, well-differentiated scattering peaks. In PdDecSi the first two peaks occupy $2\theta$ positions near the most intense peak of the type II* and type I phases, respectively. However, at higher $2\theta$ angles, there is poor resemblance of this type II phase to a superposition of the type I and II* structures. (This scenario has absolutely no merit for the type II phase of PdOctSi because of the pronounced split in the two narrow low-angle peaks of the type I phase.) As mentioned previously, a linear combination of the type II* and HCM phases is clearly inconsistent with the UV−vis absorption data. One possibility, for PdDecSi, is that a "transient" type M″-like phase forms (analogous to that in the PdOctSi progression) and persists at long times in advance of a partial transformation to the type II* structure. While this type M″ form would resemble, from an X-ray scattering perspective, the HCM (M) phase, there would necessarily be distinct differences. In particular, the *long* wavelength UV−vis absorption features would have to be associated with this phase.

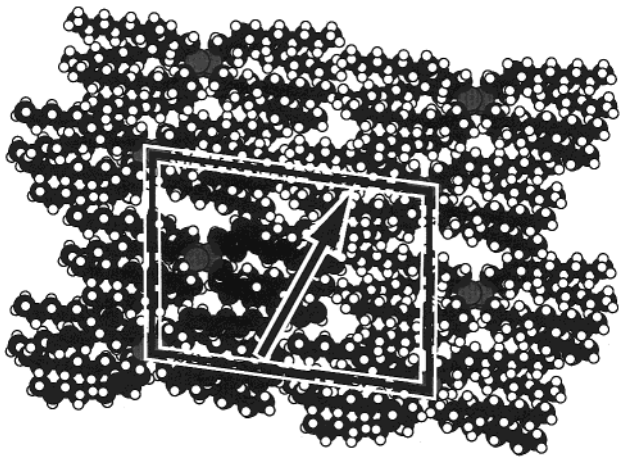

**Figure 10.** Sketch of proposed single-phase type II structure which is intermediate between the type I and type II* structures. The bold arrow shows the reorientation of the alkyl side chain ordering in this motif.

Still we note that long time annealing of the type I structure gave essentially single-phase materials in the PdDecSi NMR studies of Mueller et al.[36] X-ray diffraction patterns from comparably prepared PdDecSi films yielded results similar to that of the type I phase shown in Figure 1 (which was obtained from warming of the type II phase). Hence, another alternative is that the type II scattering pattern is dominated by a single structural phase intermediate between the two limiting cases, type I and II*. A example sketch approximating this intermediate is shown in Figure 10. Modeling (not shown) of either the PdDecSi and PdOctSi data in terms of a single structure were not as satisfactory as in the previous models although tentative unit cell parameters are given in Table 1. A transformation of this kind clearly requires large-scale translations parallel to the *a*-axis from its starting point, the type I phase, and two chains per unit cell are now necessary. The translational displacements, which are proposed for the type II → I transition, tend to reorient the interchain nesting of alkyl chains from a direction that is perpendicular to the *a*−*c* plane to, as depicted by the bold arrow Figure 10, a direction rotated by approximately 30°. This large-scale migration would be very sluggish, and this clearly correlates very well with the reported slow kinetics of the type II → I transition.

The large unit cell type III structure can also be addressed using the brick-wall-like template of Figure 8a. Tripling the unit cell along the *a*-axis direction in combination with other modest changes in the lattice parameters gives peak positions in excellent agreement with the data shown in Figure 11. All four claimed superlattice reflections can be indexed. More importantly, their relative intensity variations can also be reproduced by introducing rotational displacements of +5°, 0°, and −5° about the *c*-axis (a setting angle) in each of the three chains forming the larger unit cell. All three chains are identical otherwise. This rotation alters the alkyl chain packing so that the intensity of the $2\theta = 20°$ peak is strongly affected. It is likely that increasing the degrees of freedom by independently

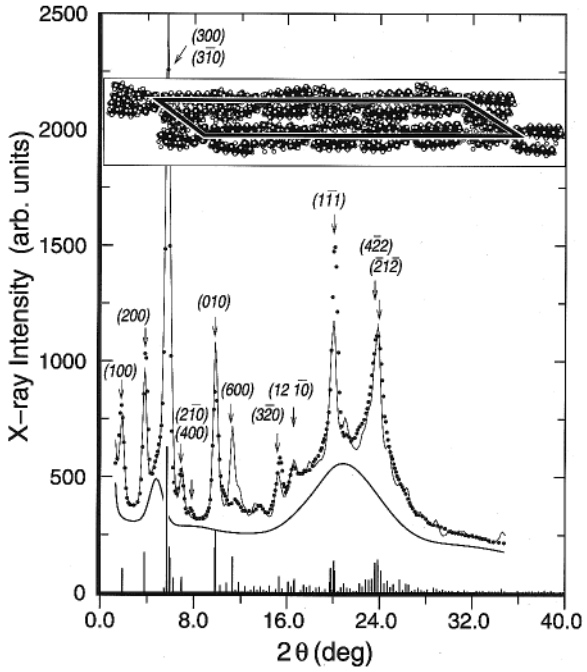


**Figure 11.** Comparison of the calculated powder profile (thin line) and experimental data (filled circles) for the type III phase of PdDecSi using the model, as viewed along the chain axes, in the inset. This figure also includes an arbitrary background profile (thick line) and the underlying Bragg contributions (as thin vertical bars).

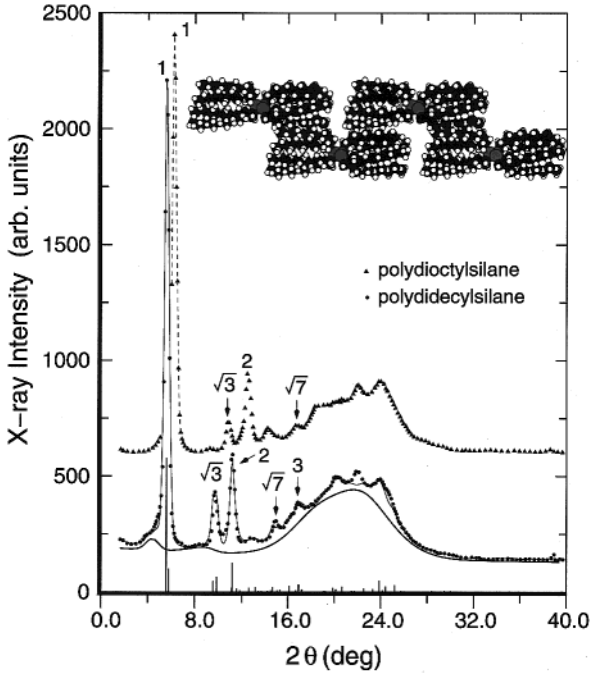


**Figure 12.** Comparison of the calculated powder profile (thin line) and experimental data (filled circles) for the QM phase of PdDecSi using the model in Figure 8a. This figure also includes an arbitrary background profile (thick line) and the underlying Bragg contributions (as thin vertical bars). The relative ratios of the PdOctSi (also a QM phase) and PdDecSi data in terms of a 2D hexagonal lattice are also shown. Inset: same model in the case of PdOctSi showing gaps at the chain ends.

altering the side chain structure within each polymer chain would significantly improve the fit to the non-equatorial scattering peaks. This reproducible large length scale uniaxial distortion of the unit cell structure is very surprising given the high level of disorder which exists within these heterogeneous materials. The specific underlying molecular-level origins for this behavior are unknown.

The QM structures, in light of their rapid cooling, include diffraction peaks whose wave vectors clearly reflect the hexagonal symmetry of the starting hexagonal columnar mesophase. As shown in Figure 12, many of these peaks exhibit wavevector ratios that map onto a 2D hexagonal lattice. Hence, it is of interest to know the extent to which the QM phase retains the structural characteristics of the preceding high-temperature phase. Despite this similarity to a hexagonal lattice, it should be recalled that only in the case of PdDecSi could rapid, deep thermal quenching lead sequentially to a type I structural motif (in PdOctSi this only occurred within a narrow temperature window). In PdDecSi the basic structural template of Figure 9a can actually be used to model the QM data by assuming a triclinic unit cell having highly anisotropic crystal coherence lengths of 20 and 10 nm and Debye temperature factors in excess of 0.1 and 0.6 $nm^2$ for the equatorial and *c*-axis directions, respectively. For PdOctSi the model template must fail at the onset (Figure 12, inset) because the requisite 2D unit cell parameter of 16.3 nm creates an unphysical interchain packing of the alkyl side chains with too much free volume appearing at the alkyl chain ends. Alternatively, if a hexagonal packing were assumed, then PdOctSi would have to undergo enormous changes in its equatorial aspect ratio in order to adopt a type I phase structure. We suggest that, in the case of PdOctSi, quenching effectively locks in the hexagonal packing of the mesophase at low temperature and that PdOctSi includes a more open (less biradial) alkyl chain packing. When combined with the secondary attribute of a far more planar backbone (as inferred by the long wavelength features in the UV−vis absorption), the exceedingly slow kinetics seen for the M′ → II transition can be rationalized by claiming more interchain entanglement of the alkyl side chains. Although speculative, there is some evidence that within the thermotropic mesophase (M) there may be distinctive differences in the alkyl chain packing between PdOctSi and PdDecSi.

## Discussion and Conclusions

The extensive polymorphism notwithstanding, this study provides insight into the subtle structure/property relationships within the $\sigma$-conjugated polysilanes and clearly identifies a hierarchal sequence of molecular level ordering processes in PdDecSi. First and foremost are the intrachain ordering of the Si backbone and the side chains. These processes dominate the structural evolution at the shortest time scales. Subsequent to these are alkyl interchain rearrangements that enhance three-dimensional order but do not alter the underlying chain packing motif. These occurs at intermediate times. The slowest structural evolution is relegated to structural transformations requiring large lateral translations of the polymer chains.

There is also strong evidence indicative of a crossover in the intrachain and interchain ordering of the alkyl side chains when progressing from a hexyl to a decyl moiety. PdOctSi can exist in either form. At temperatures above 10 °C a more open, splayed packing of the alkyl side chains dominates, while between 5 and 10 °C, there is sufficient side chain mobility to slowly

convert to the biradial "bow-tie"-shaped motif of Figure 8a. Rapid cooling, from the mesophase, below this window effectively traps the side chains in the splayed form. Clearly the specific Si backbone conformations are constrained by the organization of the side chains, and in the case of PdOctSi, a more planar conformation is achieved when the nested side chain motif of Figure 8a is suppressed. The actual thermodynamically stable low-temperature form should be the type II phase.

These processes are often, but *not* always, accompanied by concurrent changes in the optical properties. In some cases a single conformational arrangement accompanies one structural phase (e.g., the single 350 nm UV−vis absorption peak in the QM PdDecSi sample). At other times two, or possibly more, backbone conformational forms are evident. The dual peak nature of the PdOctSi QM phase UV−vis absorption supports this characteristic. More recent follow-up studies of the QM phase[59] in PdOctSi indicate that the relative peak intensity ratios are both temperature- and time-dependent. All told, there is evidence for three distinct backbone conformations in these samples, and these yield UV−vis absorption peaks centered near 350, 365, and 375 nm. The specific Si sequencing is still a mystery. All models presented in this work employ Si backbone conformations intermediate to an all-D or all-T sequence. Unfortunately, the overall contribution by the alkyl side chains to the calculated structure factors was sufficiently dominating that even a qualitative determination is precluded.

Since rapid cooling is always accompanied by the appearance of an UV−vis absorption maximum at 350 nm or *longer* wavelengths, it seems improbable that the stated hexagonal columnar mesophase includes a coil-like meandering of the silicon backbones. Large twists across gauche-like linkages would require extensive alkyl interchain interdigitation, and these would most likely dictate slower ordering kinetics. Hence, some revision in the conventional view of this hexagonal columnar mesophase may be warranted. We suggest a more nearly planar average backbone conformation with greater disorder of the alkyl side chains to "fill out" each hexagonal column. Recent studies of polysilanes in solution have also concluded that the narrow temperature range over which thermochromism changes often occurs requires structural evolution between two ordered states.[60]

There are also interesting future prospects. The clear stepwise structural progression in the PdDecSi may provide a relatively facile framework for studying the kinetics of nucleation and growth for buried metastable states. In the case of the PdOctSi the existence of a mesophase-like structure whose single UV−vis absorption maximum is red-shifted over 50 nm from that of the HCM may provide a clearer picture of the relationship between side chain ordering and the Si backbone conformation. Finally, we note that these extensive, but by no means exhaustive, observations may not have revealed all facets of the diverse polymorphic behavior in either PdOctSi or PdDecSi. Analogous studies of other closely related polysilanes or other thermochromic $\pi$-conjugated polymers are also likely to generate equally interesting results.

**Acknowledgment.** We gratefully acknowledge support of this work through NSF Grants DMR-9810623 (R.W.) and DMR-9631575 (W.C. and M.J.W.). The authors are indebted to L.W. Bruch, B.L. Farmer, M.B. Webb, and B. Wunderlich for their enlightening discussions. We also acknowledge M. Gozi and J. Truitt for their early contributions to the experimental studies.

## References and Notes

(1) Lotz, B.; Wittmann, J. C.; Lovinger, A. J. *Polymer* **1996**, *37*, 4979.
(2) Rosa, C. D.; Capitani, D.; Cosco, S. *Macromolecules* **1997**, *30*, 8322.
(3) Wang, S.; Brisse, F. *Macromolecules* **1998**, *31*, 2265.
(4) Keller, A.; Cheng, S. Z. D. *Polymer* **1998**, *39*, 4461.
(5) Cheng, S. Z. D.; Keller, A. *Annu. Rev. Mater. Sci.* **1998**, *28*, 533.
(6) Sirota, E. B.; Herhold, A. B. *Science* **1998**, *283*, 529.
(7) Leclerc, M.; Faid, K. In *The Handbook of Conducting Polymers*, 2nd ed.; Skotheim, T. A., Elsenbaumer, R. L., Reynolds, J. R., Eds.; Mercel-Dekker: New York, 1998; p 695.
(8) Yuan, C.-H.; Hoshino, S.; Toyoda, S.; Suzuki, H.; Fujiki, M.; Matsumoto, N. *Appl. Phys. Lett.* **1997**, *71*, 3326.
(9) Harrah, L. A.; Zeigler, J. M. *J. Polym. Sci., Polym. Lett. Ed.* **1985**, *23*, 209.
(10) Rabolt, J. F.; Hofer, D.; Miller, R. D.; Fickes, G. N. *Macromolecules* **1986**, *19*, 611.
(11) Rughooputh, S. D. D. V.; Hotta, S.; Hegger, A. J.; Wudl, F. *J. Polym. Sci., Polym. Phys. Ed.* **1987**, *25*, 1071.
(12) Schilling, F. C.; Lovinger, A. J.; Davis, D. D.; Bovey, F. A.; Zeigler, J. M. *Macromolecules* **1993**, *26*, 2716.
(13) Yuan, C.-H.; West, R. *Macromolecules* **1994**, *27*, 629.
(14) Obata, K.; Kira, M. *Chem. Commun.* **1998**, *12*, 1309.
(15) Oka, K.; Fujiue, N.; Dohmaru, T.; Yuan, C.-H.; West, R. *J. Am. Chem. Soc.* **1997**, *119*, 4074.
(16) Yuan, C.-H.; West, R. *Chem. Commun.* **1997**, *19*, 1825.
(17) Song, K.; Miller, R. D.; Wallraaf, G. M.; Rabolt, J. F. *Macromolecules* **1992**, *25*, 3629.
(18) West, R. In *Comprehensive Organometallic Chemisty II*; Davies, A. G., Ed.; Pergamon: Oxford, 1994; Vol. 2, Chapter on Organopolysilanes, p 77.
(19) Lacave-Goffin, B.; Hevesi, L.; Demoustier-Champange, S.; Devaux, J. *ACH−Modeles Chem.* **1999**, *136*, 214.
(20) Lovinger, A. J.; Davis, D. D.; Schilling, F. C.; Bovey, F. A.; Zeigler, J. M. *Polym. Commun.* **1989**, *30*, 356.
(21) Lovinger, A. J.; Davis, D. D.; Schilling, F. C.; Padden, F. J.; Bovey, F. A.; Zeigler, J. M. *Macromolecules* **1991**, *24*, 132.
(22) Patnaik, S. S.; Farmer, B. L. *Polymer* **1992**, *33*, 5121.
(23) Welsh, W. J.; Lin, W.; Tersigni, S. *Polym. Prepr.* **1992**, *33* (1), 673.
(24) Leites, L. A.; Yadritseva, T. S.; Bukalov, S. S.; Frunze, T. M.; Antipova, B. A.; Demet'ev, V. V. *Vysokomol. Soedin. A+* **1992**, *34*, 104.
(25) Miller, R. D.; Farmer, B. L.; Fleming, W.; Sooriyakumaran, R.; Rabolt, J. F. *J. Am. Chem. Soc.* **1987**, *109*, 2059.
(26) Schilling, F. C.; Lovinger, A. J.; Zeigler, J. M.; Davis, D. D.; Bovey, F. A. *Macromolecules* **1989**, *22*, 3055.
(27) Neumann, F.; Teramae, H.; Downing, J. M.; Michl, J. *J. Am. Chem. Soc.* **1998**, *120*, 573.
(28) Albinsson, B.; Antic, D.; Neumann, F.; Michl, J. *J. Phys. Chem.* **1999**, *103*, 2184.
(29) Fogarty, H. A.; Ottoson, C.-H.; Michl, J. *J. Mol. Struct.*, in press.
(30) Michl, J.; West, R. In *Silicon-based Polymers: The Science and Technology of their Synthesis and Applications*; Chojnowski, J., Jones, R. G., Ando, W., Eds.; Chapman and Hall: New York, 1999; Chapter on Electronic Structure and Spectroscopy of Polysilanes, in press.
(31) These two transoid forms (a double-well potential) replace the $T_0$ (anti) conformation (a single well).
(32) Rabolt, J. F.; Hofer, D.; Miller, R. D.; Ficks, G. N. *Macromolecules* **1986**, *19*, 611.
(33) Karikari, E. K.; Greso, A. J.; Farmer, B. L.; Miller, R. D.; Rabolt, J. F. *Macromolecules* **1993**, *26*, 3937.
(34) KariKari, E. K.; Farmer, B. L.; Hoffman, C. L.; Rabolt, J. F. *Macromolecules* **1994**, *27*, 7185.
(35) Bukalov, S. S.; Leites, L. A.; West, R.; Asuke, T. *Macromolecules* **1996**, *29*, 907.
(36) Mueller, C.; Frey, H.; Schmidt, C. *Monatsh. Chem.* **1999**, *130*, 175.
(37) Kanai, T.; Ishibashi, H.; Hayashi, Y.; Oka, K.; Dohmaru, T.; Ogawa, T.; Furukawa, S. *Chem. Lett.* **2000**, *6*, 650.
(38) Winokur, M. J.; Koe, J.; West, R. *Polym. Prepr.* **1997**, *38* (2), 57.

(39) Jambe, B.; Jonas, A.; Devaux, J. *J. Polym. Sci., Polym. Phys.* **1997**, *35*, 1533.
(40) Furukawa, S. *Thin Solid Films* **1998**, *331*, 222.
(41) Patnaik, S. S.; Farmer, B. L. *Polym. Prepr.* **1992**, *33* (1), 272.
(42) Patnaik, S. S.; Farmer, B. L. *Polymer* **1993**, *33*, 4443.
(43) Trefonas, P.; West, R.; Miller, R. D.; Hofer, D. *J. Polym. Sci., Polym. Lett. Ed.* **1983**, *21*, 819.
(44) Trefonas, P.; West, R. *Inorg. Synth.* **1988**, *25*, 58.
(45) Despotopoulou, M. M.; Frank, C. W.; Miller, R. D.; Rabolt, J. F. *Macromolecules* **1996**, *29*, 5797.
(46) Frank, C. W.; Rao, V.; Despotopoulou, M. M.; Pease, R. F. W.; Hinsberg, W. D.; Miller, R. D.; Rabolt, J. F. *Science* **1996**, *273*, 912.
(47) Prosa, T. Ph.D. Thesis, University of Wisconsin, 1996.
(48) Nishimura, H.; Sarko, A. *Macromolecules* **1991**, *24*, 771.
(49) The structures also form after rapid cooling to intermediate temperatures (e.g., −5 °C for type I and −25 °C for type III).
(50) Busing, W. *Macromolecules* **1990**, *23*, 4068.
(51) *Chemical Physics of Intercalation*; Bernier, P., Fischer, J. E., Roth, S., Solin, S. A., Eds.; Plenum: New York, 1993; NATO ASI Ser. Vol. B305.
(52) The PdOctSi data in this work qualitatively resemble that of ref 33, but the specific *d*-spacings are significantly different. Sample specific variations have been observed in these materials and are the likely origin of this discrepancy.
(53) Weber, P.; Guillon, D.; Skoulios, A.; Miller, R. D. *Liq. Cryst.* **1990**, *8*, 825.
(54) The PdDSi unit cell given in ref 33 requires that the two polymer chains forming the unit cell have different equatorial orientations in order that all stated reflections are allowed. Introducing this assumption creates calculated structure factors with numerous equatorial reflections having nonzero intensities. Many of these do not appear in the experimental data.
(55) Unconventional unit cells are preferred in this discussion because they better reflect the lamellar construction of the polymer host.
(56) At present is not possible to distinguish a $T_0$ from the $T_\pm$ conformations by structural refinement.
(57) Wunderlich, B. *Macromol. Symp.* **1995**, *98*, 1069. Wunderlich, B. *Adv. Polym. Sci.* **1988**, *87*, 1.
(58) Abdallah, D. J.; Bachman, R. E.; Perlstein, J.; Weiss, R. G. *J. Phys. Chem.* **1999**, *103*, 9269.
(59) Chunwachirasiri, W.; et al., to be published.
(60) Sanji, T.; Sakamoto, K.; Sakurai, H.; Ono, K. *Macromolecules* **1999**, *32*, 3788.

MA9919716